ELSEVIER

Biophysical Chemistry 125 (2007) 159–165

Biophysical Chemistry

http://www.elsevier.com/locate/biophyschem

Self-association of adrenodoxin studied by using analytical ultracentrifugation

Joachim Behlke [a,*], Otto Ristau [a], Eva-Christina Müller [a], Frank Hannemann [b], Rita Bernhardt [b]

[a] *Max Delbrück Center for Molecular Medicine, 13092 Berlin, FRG*
[b] *Universität des Saarlandes, Fachbereich Biochemie, 66041 Saarbrücken, FRG*

Received 16 May 2006; received in revised form 19 July 2006; accepted 19 July 2006
Available online 17 August 2006

Abstract

The mitochondrial steroid hydroxylase system of vertebrates utilizes adrenodoxin (Adx), a small iron–sulfur cluster protein of about 14 kDa as an electron carrier between a reductase and cytochrome P450. Although the crystal structure of this protein has been elucidated, the solution structure of Adx was discussed contrary in the literature [I.A. Pikuleva, K. Tesh, M.R. Waterman, Y. Kim, The tertiary structure of full-length bovine adrenodoxin suggests functional dimers, Arch. Biochem. Biophys. 373 (2000) 44–55; D. Beilke, R. Weiss, F. Löhr, P. Pristovsek, F. Hannemann, R. Bernhardt, H. Rüterjans, A new electron mechanism in mitochondrial steroid hydroxylase systems based on structural changes upon the reduction of adrenodoxin, Biochemistry 41 (2002) 7969–7978]. Therefore, it was necessary to study the self-association of this protein by using analytical ultracentrifugation over a larger concentration range. As could be demonstrated in sedimentation velocity experiments, as well as sedimentation equilibrium runs with explicit consideration of thermodynamic non-ideality, the full-length protein (residues 1–128) in the oxidized state resulted in a monomer–dimer equilibrium ($K_a \sim 3 \times 10^2$ M^{-1}). For truncated Adx (1–108), as well as the reduced Adx, the association behavior was strongly reduced. The consequences of this behavior are discussed with respect to the physiological meaning for the Adx system.

Keywords: Sedimentation velocity; Sedimentation equilibrium; Self-association; Association constants; Thermodynamic non-ideality

1. Introduction

Iron sulfur proteins belong to a distinct protein class and are widely distributed in bacteria, plants and animals [1]. Mostly ferredoxins contain either a [4Fe–4S] cluster or a [2Fe–2S] cluster by which these proteins take part in electron transfer reactions [1,2]. As part of the mitochondrial steroid hydroxylase system of vertebrates the [2Fe–2S] ferredoxins transfer one electron from an NAD(P)H dependent reductase to different cytochromes P450. Some bacterial [2Fe–2S] ferredoxins share similar functions. Adrenodoxin (Adx), the shuttle protein in the adrenal cortex, is a soluble low molecular mass protein of 14 kDa. Recently, the X-ray crystal structures of a truncated form [3] as well as wild-type protein of Adx [4] and a complex of Adx with the natural electron donor adrenoxin reductase [5] were analyzed. Furthermore, molecular regions and distinct amino acids, which are involved in the interaction with reductase and P450, were determined using the techniques of chemical modification [6], cross-linking [7] and site-directed mutagenesis [8–10].

To describe the mechanism of the electron transfer reactions by Adx, a cluster and a shuttle mechanism have been proposed [11,12]. Cluster models either invoking a ternary complex [13] or a quaternary complex with two molecules of Adx, one reductase and one P450 molecule have been discussed [14,15]. The shuttle mechanism considers Adx as a mobile electron carrier between reductase and P450 supported by the fact that the dissociation constant for the complex Adx-reductase is enhanced more than 20 times by reduction [16]. Recently, a mechanism proceeding via a modified shuttle mechanism was proposed, with both monomers and dimers acting as electron

* Corresponding author. Tel.: +49 30 9406 2205/2802; fax: +49 30 9406 2802.
E-mail address: behlke@mdc-berlin.de (J. Behlke).

0301-4622/$ - see front matter © 2006 Elsevier B.V. All rights reserved.
doi:10.1016/j.bpc.2006.07.011

carriers, as deduced from the observation that oxidized Adx can form dimers in cross-linking experiments [17]. Furthermore, molecular mass values clearly higher than that of the monomer were found in light scattering studies [4]. Surprisingly, these authors found higher molecular masses at lower Adx concentrations (1.37 mg/ml) and lower molecular masses at higher concentrations (10 mg/ml). This behavior seems to violate Le Chatelier's principle and can be explained partially by considering the thermodynamic non-ideality in such high concentrations. Therefore, it was necessary to repeat such experiments using analytical ultracentrifugation allowing to consider the influence of virial coefficients on the self-association of proteins [18]. Here we describe studies of Adx and a shorter variant of this protein Adx (4–108) with respect to the dimerization behavior using sedimentation equilibrium and sedimentation velocity experiments in an analytical ultracentrifuge. Some additional experiments were also carried out with reduced Adx.

2. Materials and methods

Adrenodoxin was prepared as described earlier [19]. Besides the wild-type protein consisting of 128 amino acids, also a shorter form comprising amino acids 4–108 (truncated Adx) was used in the studies (see [20]). Moreover, reduced Adx was obtained by careful addition of sodium dithionite. Protein concentration was determined using an extinction coefficient of 1.1×10^4 M^{-1} cm^{-1} at 414 nm [21]. Only electrophoretically pure proteins were used in the experiments. The mass spectrometric molecular weight determination (Q-Tof1, Micromass, Manchester, UK) gave a molecular mass of the purified recombinant Adx that corresponds exactly to the sequence encoded by the cDNA without heterogeneity due, for example, to the partial hydrolysis of the C-terminus. For further experiments, the samples were dissolved in 10 mM K-phosphate buffer, pH 7.4, containing 0.3 M NaCl.

Molecular mass and self-association studies on the proteins were carried out by using an analytical ultracentrifuge XL-A (Beckman, Palo Alto, CA). Sedimentation equilibrium experiments were performed for the direct calculation of the association constants based on the increased molecular mass. About 300 µl solute graduated in different concentrations were loaded into seven standard double sector cells and centrifuged for 2 h at 24,000 rpm (overspeed) followed by 70–100 h equilibrium speed at 20,000 rpm and 10 °C. In each experiment, the records were manifold repeated and compared to be sure the sedimentation equilibrium was ascertained. The radial concentration distributions in each run were recorded at wavelengths between 414 and 640 nm depending on the concentration used in the experiments. This wavelength interval contains no steep region, which can falsify the absorption measurement. In order to study the association behavior in solutions of high protein concentration, non-ideality had to be considered and as mentioned earlier [22–24,18] the thermodynamic analysis of solutions at high protein concentration is difficult because the concentration power series may not converge. Recently, we developed an approach to overcome this problem by fitting the following equation to the data

$$c_r = z + (K_2 - 2B_{20})z^2 + \left(K_3 + 6B_{20}^2 - \frac{3}{2}B_{30} - \frac{3}{2}B_{11}K_2\right)z^3 + \left(12B_{20}B_{30} - \frac{64}{3}B_{20}^3 - \frac{4B_{40}}{3} + K_2\left(4B_{11}B_{20} + B_{11}^2 - B_{21}\right) - K_2^2B_{02} - \frac{4}{3}K_3B_{101}\right)z^4 \quad (1)$$

with

$$z = z_0\exp\left(\frac{M(1-\bar{v}\rho_0)\omega^2(r^2-r_0^2)}{2RT}\right) \quad (2)$$

Here c is the weight concentration in g/l, and K_2 and K_3 are the association constants for dimer and trimer formation. The B symbols (describing the excluded volume caused by the collision processes) are the true statistically defined virial coefficients [25]. The first index defines the number of monomers, the second index the number of dimers and the third index the number of trimers in the collision process. The activity of the monomers, z, calculated from the activity at the reference radius, was obtained from the so-called ψ function [26]. B_{20} is the known second virial coefficient. Since it is impossible to estimate the higher virial coefficients directly, these were calculated according to Boublik and Nezbeda [27] and defined as multiples of B_{20} valid for uncharged molecules and known shape. In all experiments, the influence of charge on the virial coefficients was excluded by addition of an appropriate amount of NaCl. Eq. (1) has the additional advantage of being explicit in concentration. Simple integration of this expression yields the theoretical loading concentration for the sector cells.

$$c_L = \frac{2}{r_b^2 - r_m^2}\int_{r_m}^{r_b} c_r \cdot r\,dr. \quad (3)$$

A program VIRIAL was written to fit the experimental data. It is able to fit simultaneously seven concentration profiles of different loading concentrations. These were obtained from a sedimentation equilibrium run using an eight-hole rotor. In order to reduce the number of fitting parameters, the effective loading concentration of each cell was calculated by numerical integration of the selected part of the radial concentration distribution. From this, the reference concentration of each cell was determined. The extinction coefficient for the chosen wavelength was derived from the records obtained at 3000 rpm and the known concentration of the protein. This technique is called signal conservation [28] was first developed by Minton [29].

Additional sedimentation velocity experiments were performed. About 400 µl Adx at different concentrations were centrifuged in standard 12 mm double sector cells at 50,000 rpm. The radial absorbance distributions were recorded at a wavelength of 415 nm at 2-min intervals.

A program LAMMNUM [30] with numerical solution of the Lamm equation according to Claverie et al. [31], Cox and Dale [32] and Schuck [33] was written. It allows the user to estimate ideal equilibrium constants (K_b) and the position of the meniscus (r_m) and cell base (r_b). LAMMNUM can also take into

account the concentration dependence of the sedimentation coefficients given by

$$s_c = s_0/(1 + k_s c) \tag{4}$$

with s_c the sedimentation coefficient at concentration c and s_0 at infinite dilution. A negative sign of k_s is diagnostic of mass interaction [34]. The program works with numerical calculated derivatives according to Todd and Haschemeyer [35]. The parameters (K_b, k_s) were introduced into the Claverie scheme according to Schuck [33]. This scheme uses the constituent sedimentation and diffusion coefficients defined by Steiner [36] and Cox [37]. To achieve more numerical stability, the dependence of the sedimentation (s_n) or diffusion (D_n) coefficients on the degree of association, n, is described by the well-known relations for spherically shaped complexes. To enhance the variability other exponent p, such as 2/3 can be chosen but not estimated by fitting. The constituent (weight average) sedimentation coefficient is

$$s(c_w) = S_M \frac{1 + \sum_2^n n^p K_n c_M^{n-1}}{1 + \sum_2^n K_n c_M^{n-1}} \tag{5}$$

for the constituent (gradient average) diffusion coefficient it follows that

$$D(c_w) = D_M \frac{1 + \sum_2^n n^p K_n c_M^{n-1}}{1 + \sum_2^n n K_n c_M^{n-1}} \tag{6}$$

c_M means the weight concentration of monomers, which can be calculated from the total concentration at each radial point by using the law of mass action. The program allows the introduction of the molecular weight and calculates the diffusion constant from the current sedimentation coefficient during the fit. Additionally, the frictional ratio can be introduced to calculate the sedimentation coefficient. If the sedimentation coefficient is held constant, the number of estimated parameters is reduced by two (s=sedimentation coefficient, D=diffusion coefficient). The excluded volume of Adx was derived from the diffusion coefficient obtained in dilute solution. D is related to the Stokes radius (R_s) as follows,

$$R_s = kT/6\pi\eta D \tag{7}$$

with k the Boltzmann constant and η the dynamic viscosity of the solvent. B_{20}, here the excluded volume, was determined according to Wills and Winzor [38] from the particle radius (R_s), the molecular mass (M) and Avogadro's number (N_A) according to Eq. (8).

$$B_{20} = 16\pi R_s^3 N_A/3M. \tag{8}$$

A program Cox was written and used to generate synthetic concentration profiles. The binding constant and the concentration dependence of s (Eq. (4)) were again introduced according to Schuck [33].

When using our program LAMMNUM to estimate binding constants without consideration of the concentration dependence of sedimentation coefficients (Eq. (4)) one estimates clearly to low bottom radii [39]. To avoid interference aggregates, we have limited the fit region near behind the crossing point that is the radius position near the cell base where the concentration profiles of the different solute concentrations intersect. Additionally, we limited the maximal absorbance to a value scarcely over the plateau level.

To describe the apparent molecular mass of dimers and momomers, the scaled particle theory of Gibbons [40] is excellently suited to higher concentrations because this theory offers a closed equation for the virial coefficients. The shape of the dimers was approximated by a prolate spherocylinder with a volume twice that of the monomer. Assuming the monomers as spheres, their volume is exact a quarter of the virial coefficient B_{20} calculated by Eq. (8). The breadth of the spherocylinder corresponds to the diameter of the monomer the length is 5/3 times the diameter. The osmotic pressure (π) of spherical particles is described by

$$\frac{\pi}{RT} = \frac{c}{1 - vc} + \frac{3vc^2}{(1 - vc)^2} + \frac{3v^2c^3}{(1 - vc)^3} \tag{9}$$

where v is the volume of the spherical monomer.

With the help of the Gibbs–Duhem equation, the partial chemical potential of the solute (μ) is given by

$$\mu = RT\left(\ln(c) - \ln(1 - vc) + \frac{1}{1 - vc} - \frac{3}{2(1 - vc)^2} + \frac{3}{(1 - vc)^3}\right). \tag{10}$$

The centrifuge equation [41] now reads

$$c_r = c_0 \exp\left(M_r(r^2 - r_0^2) - \ln(\gamma)\right) \tag{11}$$

with

$$\ln(\gamma) = \frac{1}{1 - vc} - \frac{3}{2(1 - vc)^2} + \frac{3}{(1 - vc)^3} - \frac{1}{1 - vc_0} + \frac{3}{2(1 - vc_0)^2} - \frac{3}{(1 - vc_0)^3} - \ln\left(\frac{1 - vc}{1 - vc_0}\right). \tag{12}$$

For the apparent molecular weight $M_{app} = \dfrac{\partial \ln(c_r)}{\partial r^2}$ follows by derivation from Eqs. (11) and (12)

$$M_{app} = \frac{M}{1 + vc\left(\frac{1}{(1-vc)} + \frac{1}{(1-vc)^2} - \frac{3}{(1-vc)^3} + \frac{9}{(1-vc)^4}\right)} \tag{13}$$

The osmotic equation for prolate spherocylinders (dimers) reads

$$\frac{\pi}{RT} = \frac{c}{1 - v_D c} + \frac{10v_D c^2}{3(1 - v_D c)^2} + \frac{100v_D^2 c^3}{27(1 - v_D c)^3} \tag{14}$$

where v_D is the volume of the dimers. Then

$$\ln(\gamma) = \frac{1}{1 - v_D c} - \frac{20}{9(1 - v_D c)^2} + \frac{100}{27(1 - v_D c)^3} - \frac{1}{1 - v_D c_0} + \frac{20}{9(1 - v_D c_0)^2} - \frac{100}{27(1 - v_D c_0)^3} - \ln\left(\frac{1 - v_D c}{1 - v_D c_0}\right) \tag{15}$$

and the apparent molecular weight of the prolate spherocylinders (dimers) is given by

$$M_{\mathrm{app,D}} = \frac{M_{\mathrm{D}}}{1 + \nu_{\mathrm{D}} c\left(\frac{1}{(1-\nu_{\mathrm{D}}c)} + \frac{1}{(1-\nu_{\mathrm{D}}c)^2} - \frac{40}{9(1-\nu_{\mathrm{D}}c)^3} + \frac{100}{9(1-\nu_{\mathrm{D}}c)^4}\right)}. \quad (16)$$

If weight concentrations g/l are used for v and also for v_{d}, the same excluded volume l/g can be applied.

3. Results

3.1. Sedimentation equilibrium

In order to study the self-association of Adx, regarding to the virial effects, sedimentation equilibrium experiments were carried out. The radial concentration distributions were recorded at 640 nm and transferred into weight concentrations based on an absorbance of 0.10908 for 1 g/l at this wavelength (see Fig. 1). The curves covering a concentration range of a few μg/ml at the meniscus up to about 12 g/l near the cell base were fitted globally using Eqs. (1) and (2) using a molecular mass of 14,190 Da for the monomeric protein.

3.1.1. Adrenodoxin

The association constant for the dimerization event was found to be $K_{\mathrm{a}}=(0.038\pm0.006)$ g/l or $(2.7\pm0.4)\cdot10^2$ M^{-1} at 10 °C. This parameter was obtained by using a value of $B_{20}=0.0058\pm0.00014$ g/l which should correspond to the excluded volume of Adx and is similar to that value derived from D and R_{s} (Eq. (8)). This value corresponds to 8 times the partial specific volume or four times the 'swollen' volume [42]. Caused by the weak binding coefficient the virial coefficient B_{20} cannot estimate directly as additional fitting parameter [43] with suitable accuracy [18]. Without consideration of virial coefficients, the association constants (K_{a}) are considerably diminished $K\approx(8\pm3)$ M^{-1}.

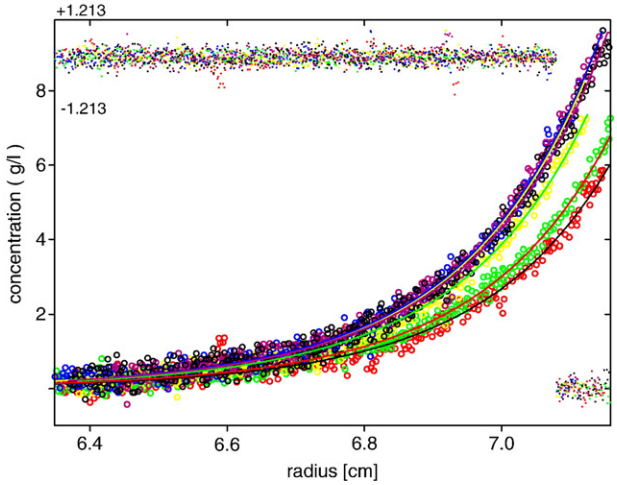

Fig. 1. Radial concentration distribution curves of Adx in 10 mM K-phosphate buffer, pH 7.4, containing, 0.3 M NaCl. The profiles with loading concentrations between 1.4 and 2.4 g/l were recorded after 72 h equilibrium speed at 20,000 rpm at 10 °C and a wavelength of 640 nm. The curves were fitted using Eq. (2).

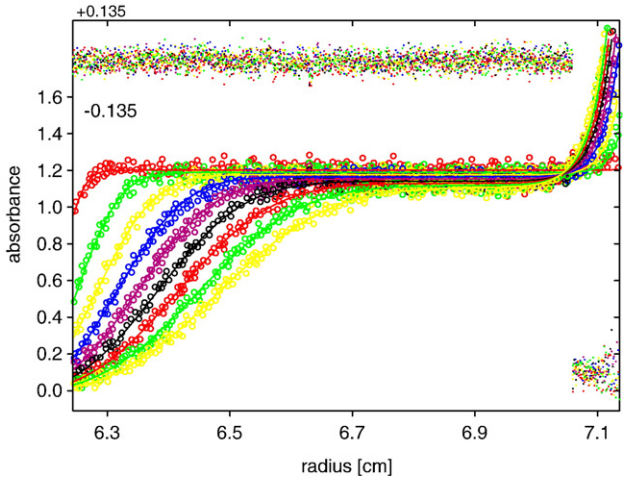

Fig. 2. Radial absorbance distributions (symbols) and fits to the data (curves) of 1.4 g/l Adx in 10 mM K-phosphate buffer, pH 7.4, containing 0.3 M NaCl. The profiles were recorded at 415 nm at time intervals of 8 min. The temperature was 20 °C and the speed 50,000 rpm. Only each second record is shown. Residuals are given in 1.6-fold amplification compared to the radial absorbance distributions.

3.1.2. Adrenodoxin (4–108) truncated

In order to estimate the influence of the C-terminal amino acids on the association of Adx (4–108) corresponding experiments with this protein were carried out. In sedimentation equilibrium with considering the thermodynamic non-ideality, clearly lower association constants were determined indicating that the C-terminal amino acids are involved in the self-association of Adx. From experiments with a concentration range between 1.8 and 7.0 g/l, an average association of $K_{\mathrm{a}}=32$ M^{-1} was deduced (not shown).

3.2. Sedimentation velocity

3.2.1. Adrenodoxin

In order to recognize the behavior of Adx, at first velocity runs obtained at 50,000 rpm were analyzed with our LAMM [44] program. Fig. 2 demonstrates a limited number of whole-boundary radial concentration distributions from the 23, which were recorded at 600-s intervals. A molecular mass of 14.8 kDa was determined somewhat higher than the theoretical value (14.19 kDa) indicating that only a few dimers exist in equilibrium with monomers. Additionally, we used our program LAMMNUM to determine the dependence of the sedimentation constant on concentration. We found a negative value ($k_{\mathrm{s}}=-0.0008$) indicative of slight mass interaction [34]. Another possibility to recognize dimers is the sedimentation distribution, which uses differentiated profiles. But tests with simulated curves generated with our program COX shows that no usable shoulder or peaks occur with such low sedimentation constants ($s<1.8$ S). That indicates that the generation of a $g^*(s)$ plot in such cases does not provide reliable information regarding protein association. With LAMMNUM and the fit procedure

described in Materials and methods, we found an ideal association constant of 89±40 M^{-1}. For sedimentation velocity experiments, the consideration of non-ideality is not possible. Such low association constants were also found in sedimentation equilibrium experiments when virial coefficients were neglected.

The known molecular mass M_1=14.19 kDa was used as a numerical constraint for the fitting. The estimation of equilibrium constants from sedimentation velocity experiments works well for dilute solutions and moderate association constants. The sedimentation and diffusion constant were determined to be s=1.52±0.05 S and $D=(9.9\pm0.2)\cdot10^{-7}$ cm^2/s.

3.2.2. Adrenodoxin (4–108) truncated

In sedimentation equilibrium analysis accounting for thermodynamic non-ideality gave clearly lower association constants indicating that the C-terminal amino acids are involved in the self-association of Adx. With sedimentation velocity, no significant binding constant was found as expected from the low value obtained in equilibrium runs. Indeed when neglecting virial coefficients in such calculations an association constant near zero results (K<10).

3.2.3. Reduced adrenodoxin

Occasion on the low temporally stability of reduced Adx (less than about 48 h) only sedimentation velocity runs were carried out. With our program LAMMNUM, no significant self-association was found.

4. Discussion

We have studied the association behavior of dissolved Adx by sedimentation-velocity ultracentrifugation to determine the type of associates formed and by sedimentation equilibrium runs to determine the affinity of the interaction under conditions of thermodynamic non-ideality. Whereas the truncated mutant Adx (4–108) has only an extremely weak tendency to associate (K_a=32 M^{-1}) wild-type Adx forms dimers with moderate affinity $K_a=(2.7\pm0.4)\cdot10^2$ M^{-1}. The main difference in the association behavior between both species seems to be caused by the C-terminal amino acids.

The tendency of Adx to self-associate in solution was proposed in the literature by several groups [4,17,13]. This was concluded from molecular mass studies by size exclusion chromatography, electrophoretic mobility and light scattering at different loading concentrations or derived from X-ray crystal structure analysis. Light scattering studies on Adx [4] yield high average molecular weights (about 23 kDa) suggesting strong dimer formation. On the other hand, their finding that the monomer−dimer equilibrium is shifted toward dimer formation when the ionic strength is increased and toward monomers when the Adx concentration is increased seems to be surprising. Clearly, the effects of thermodynamic non-ideality in interpretation of their results were ignored. Studies on biopolymers with hydrodynamic, scattering or other physico-chemical methods yield expected molecular parameters only in dilute solutions. In concentrated protein solutions higher than about 2 g/l, one has to consider the thermodynamic non-ideality caused by charge effects and the exclusion volume. This leads to a distinct reduction of the apparent molecular mass and other molecular parameters. Indeed, the apparent molecular masses of dissolved molecules decrease due to virial effects. Whereas the charge effect can be neglected by addition of an appropriate amount of neutral salts, the excluded volume is a defined value of each molecule and has to be considered, especially at higher concentrations. Based on the averaged association constant $K_a=(2.7\pm0.4)\cdot10^2$ M^{-1} and a B_{20}=0.0058 g/l, we have calculated the apparent molecular masses of Adx. As seen in Fig. 3, the apparent molecular masses of Adx increase as expected with increasing concentrations, however, only up to about 4 g/l. Although the concentration of dimers increases furthermore, the apparent molecular mass values decrease at higher protein concentrations due to the influence of the excluded volume. Additional plotted curves for pure Adx monomers and dimers show a negative, but non-linear concentration dependence of the apparent molecular masses (Fig. 3). The curves based on self-association and dimeric Adx moved closer together at higher concentrations.

Exact data to describe the solution structure of Adx with respect to its reliable association behavior are missing. An important precondition is the use of a pure functional Adx free of by-products. In this communication, we present thermodynamically exact equilibrium constants that describe unequivocally the association behavior of Adx and the mutated form of Adx (4–108) in solution over a large concentration range and in a solution of moderate ionic strength that corresponds to physiological conditions. The association constants for a monomer–dimer equilibrium communicated here are small and explain why self-association is only apparent at high concentrations (e.g. 12 g/l) (Fig. 3). For the reduced Adx, no significant self-association could be observed.

Estimated association constants without consideration of the thermodynamic non-ideality for Adx so far communicated [4] are clearly different from the parameters derived in the present

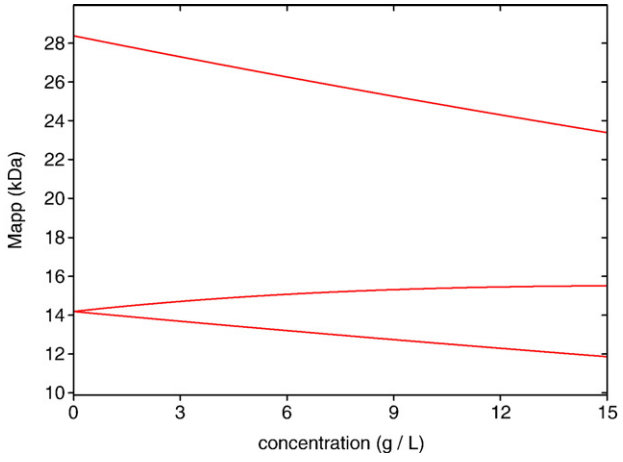

Fig. 3. Influence of the concentration on the apparent molecular masses (M_{APP}) of wt-adx derived from the association constant $K_a=2.7\cdot10^2$ M^{-1} obtained at 10 °C using a virial coefficient B_{20}=0.0058 g/l (middle curve). The upper and lower lines represent the corresponding molecular masses for $K_a=\infty$ (only dimers) or K_a=0 (only monomers), respectively.

study and not understandable from the physicochemical point of view. Surprisingly, strong dimerization was found at low concentrations, violating Le Chatelier's principle.

The association behavior of Adx described in this study is in good agreement with the electron shuttle mechanism described first by Lambeth et al. [12] and the advanced modified shuttle mechanism suggested by Beilke et al. [17]. According to the shuttle model, Adx serves as a mobile carrier between Adx-reductase and different cytochromes P450. In the oxidized form, an equilibrium between monomers and dimers is present, whereas upon reduction conformational changes in the C-terminal contact region lead to the dissociation of the homodimer. This is important for the physiological function because a freely accessible C-terminus participates in the cytochrome P450 binding [20,45]. In addition, the association behavior of Adx indicates that the amount of dimers increases at higher protein concentrations, which may accelerate the loading of the Adx molecules in the Adx-reductase-Adx complex under conditions of high steroid biosynthetic activity of the mitochondria because the number of association and dissociation events will be reduced significantly.

Acknowledgement

The authors are grateful to Drs. U. Heinemann and J.J. Müller, MDC Berlin for supporting and critical reading the manuscript. This work was supported by grants from the DFG (Be 1343/12-3) and the Fonds der Chemischen Industrie.

References

[1] R. Bernhardt, Cytochrome P450: structure, function, and generation of reactive oxygen species, Rev. Physiol. Pharmacol. 127 (1995) 137–221.
[2] H. Beinert, R.H. Holm, E. Münck, Iron sulfur clusters: nature's modular, multipurpose structures, Science 277 (1997) 653–659.
[3] A. Müller, J.J. Müller, Y.A. Muller, H. Uhlmann, R. Bernhardt, U. Heinemann, New aspects of electron transfer revealed by the crystal structure of a truncated bovine adrenodoxin, Adx (4–108), Structure 6 (1998) 269–280.
[4] I.A. Pikuleva, K. Tesh, M.R. Waterman, Y. Kim, The tertiary structure of full-length bovine adrenodoxin suggests functional dimers, Arch. Biochem. Biophys. 373 (2000) 44–55.
[5] J.J. Müller, A. Lapko, G. Bourenko, K. Ruckpaul, U. Heinemann, Adrenodoxin reductase–adrenodoxin complex structure suggests electron Transfer path in steroid biosynthesesis, J. Biol. Chem. 276 (2001) 2786–2789.
[6] L.M. Geren, O.P. Brien, J. Stonehuerner, F. Millett, Identification of specific carboxylate groups on adrenodoxin that are involved in the interaction with adrenodoxin reductase, J. Biol. Chem. 259 (1984) 2155–2160.
[7] E.-C. Müller, A. Lapko, A. Otto, J.J. Müller, K. Ruckpaul, U. Heinemann, Covalently crosslinked complexes of bovine adrenodoxin with adrenodoxin reductase and cytochrome P450scc. Mass spectrometry and Edman degradation of complexes of the steroidogenic hydrolase system, Eur. J. Biochem. 268 (2001) 1837–1843.
[8] V.M. Coghlan, L.E. Vickery, Site-specific mutations in human ferrodoxin that affect binding to ferredoxin reductase and cytochrome P450scc, J. Biol. Chem. 266 (1991) 18606–18612.
[9] A. Wada, M.R. Waterman, Identification by site-directed mutagenesis of two lysine residues in cholesterol side chain cleavage cytochrome P450 that are essential for adrenodoxin binding, J. Biol. Chem. 267 (1992) 22877–22882.
[10] F. Hannemann, M. Rottmann, B. Schiffer, J. Zapp, R. Bernhardt, The loop region covering the iron–sulfur cluster in bovine adrenodoxin comprises a new interaction site for redox partners, J. Biol. Chem. 276 (2001) 1369–1375.
[11] I. Hanukoglu, C.T. Privalle, C.R. Jefcoate, Mechanisms of ionic activation of adrenal mitochondrial cytochromes P-450$_{SCC}$ and P-45011β, J. Biol. Chem. 256 (1981) 4329–4335.
[12] J.D. Lambeth, D.W. Seybert, J.R. Lancaster, J.C. Salerno, H. Kamin, Steroidogenic electron transport in adrenal cortex mitochondria, Mol. Cell. Biochem. 45 (1982) 13–31.
[13] T. Kido, T. Kimura, The formation of binary and ternary complexes of cytochrome P450scc with adrenodoxin and adrenodoxin reductase–adrenodoxin complex. The implication in ACTH function, J. Biol. Chem. 254 (1979) 11806–11815.
[14] T. Hara, T. Kumura, Active complex between adrenodoxin reductase and adrenodoxin in the cytochrome P450scc reduction reaction, J. Biochem. 105 (1989) 601–605.
[15] T. Hara, C. Koba, M. Takeshima, Y. Sagara, Evidence for the cluster model of mitochondrial steroid hydroxylase system derived from dissociation constants of the complex between adrenodoxin reductase and adrenodoxin, Biochem. Biophys. Res. Commun. 276 (2000) 210–215.
[16] J. Lambeth, O.S. Pember, Cytochrome P450scc adrenodoxin complex. Reduction properties of the substrate-associated cytochrome and relation of the reduction states of heme and iron–sulfur centers, J. Biol. Chem. 258 (1983) 5596–5602.
[17] D. Beilke, R. Weiss, F. Löhr, P. Pristovsek, F. Hannemann, R. Bernhardt, H. Rüterjans, A new electron mechanism in mitochondrial steroid hydroxylase systems based on structural changes upon the reduction of adrenodoxin, Biochemistry 41 (2002) 7969–7978.
[18] J. Behlke, O. Ristau, Analysis of protein self-association under conditions of the thermodynamic nonideality, Biophys. Chemist. 87 (2000) 1–13.
[19] H. Uhlmann, V. Beckert, D. Schwarz, R. Bernhardt, Expression of bovine adrenodoxin in *E. coli* and site-directed mutagenesis of /2Fe–2S/ cluster ligands, Biochem. Biophys. Res. Commun. 188 (1992) 1131–1138.
[20] H. Uhlmann, R. Kraft, R. Bernhardt, C-terminal region of adrenodoxin affects its structural integrity and determines differences in its electron transfer function to cytochrome P-450, J. Biol. Chem. 269 (1994) 22557–22564.
[21] J.J. Huang, T. Kimura, Studies on adrenal steroid hydroxylases. Oxidation–reduction properties of adrenal iron–sulfur proteins, Biochemistry 12 (1973) 404–409.
[22] T.J. Hill, Y.D. Chen, Theory of aggregation in solution: I. General equations and application to the stacking of bases, nucleosides, etc. Biopolymers 12 (1973) 1285–1312.
[23] P.R. Wills, M.P. Jacobsen, D.J. Winzor, Direct analysis of solute self-association by sedimentation equilibrium, Biopolymers 38 (1996) 119–130.
[24] P.R. Wills, D.J. Winzor, Studies of solute self-association by sedimentation equilibrium: allowance for effects of thermodynamic non-ideality beyond the consequences of nearest-neighbor interactions, Biophys. Chemist. 91 (2001) 253–262.
[25] W.G. McMillan, J.E. Mayer, The statistical thermodynamics of multi-component systems, J. Chem. Phys. 13 (1945) 276–305.
[26] D.J. Winzor, M.P. Jacobsen, P.R. Wills, Allowance for the thermodynamic nonideality in the analysis of sedimentation equilibrium distributions reflecting complex formation between dissimilar reactants, Prog. Colloid & Polym. Sci. 113 (1999) 69–75.
[27] T. Boublik, I. Nezbeda, P–V–T behaviour of hard body fluids. Theory and experiment, Collect. Czechoslov. Chem. Commun. 51 (1986) 2301–2432.
[28] J.S. Philo, Sedimentation equilibrium analysis of mixed associations using numerical constrains to impose mass or signal conservation, Methods Enzymol. 321 (2000) 100–120.
[29] A.P. Minton, Conservation of signal: a new algorithm for the elimination of the reference concentration as an independently variable parameter in the analysis of sedimentation equilibrium, in: T.M. Schuster, T.M. Laue (Eds.), Modern Analytical Ultracentrifugation, Birkhauser, Boston, MA, 1994, pp. 81–93.
[30] J. Behlke, O. Ristau, LAMMNUM: a program to study self-associating macromolecules in sedimentation velocity experiments, in: D.J. Scott, S.E.

Harding, A.J. Rowe (Eds.), Analytical Ultracentrifugation, Techniques and Methods, Royal Society of Chemistry, Cambridge, 2005, pp. 122–132.
[31] J.-M. Claverie, H. Dreux, R. Cohen, Sedimentation of generalized systems of interacting particles: I. Solution of systems of complete Lamm equations, Biopolymers 14 (1975) 1685–1700.
[32] D.J. Cox, R.S. Dale, Simulation of transport experiments for interacting systems, in: C. Frieden, L.W. Nichol (Eds.), Protein–Protein Interaction, Wiley, New York, 1981, pp. 173–201.
[33] P. Schuck, Sedimentation analysis of noninteracting and self-associating solutes using numerical solutions of the Lamm equation, Biophys. J. 75 (1998) 1503–1512.
[34] T.M. Laue, B.D. Shah, T.M. Ridgeway, S.L. Pelletier, Computer-aided interpretation of analytical sedimentation data for proteins, in: S.E. Harding, A.J. Rowe, J.C. Horton (Eds.), Analytical Ultracentrifugation in Biochemistry and Polymer Science, Royal Society, Cambridge, 1992, pp. 90–125.
[35] G.P. Todd, R.H. Haschemeyer, General solution to the inverse problem of the differential equation of the ultracentrifuge, Proc. Natl. Acad. Sci. U. S. A. 78 (1981) 6739–6743.
[36] R.F. Steiner, Reversible association processes of globular proteins: V. The study of associating systems by the methods of macromolecular physics, Arch. Biochem. Biophys. 49 (1954) 400–416.
[37] D.J. Cox, Computer simulation of sedimentation in the ultracentrifuge: IV. Sedimentation of self-associating solutes, Arch. Biochem. Biophys. 129 (1969) 106–123.
[38] P.R. Wills, D.J. Winzor, Thermodynamic non-ideality and sedimentation equilibrium, in: S.E. Harding, A.J. Rowe, J.C. Horton (Eds.), Analytical Ultracentrifugation in Biochemistry and Polymer Science, Royal Society, Cambridge, 1992, pp. 311–330.
[39] J. Behlke, O. Ristau, A new possibility to recognize the concentration dependence of sedimentation coefficients, Prog. Colloid & Polym. Sci. 131 (2006) 29–32.
[40] R.M. Gibbons, The scaled particle theory for particles of arbitrary shape, Mol. Phys. 17 (1969) 81–86.
[41] H. Fujita, Mathematical Theory of Sedimentation Analysis, Academic Press, New York, 1962.
[42] A.J. Rowe, The concentration dependence of sedimentation, in: S.E. Harding, A.J. Rowe, J.C. Horton (Eds.), Analytical Ultracentrifugation in Biochemistry and Polymer Science, Royal Society, Cambridge, 1992, pp. 394–406.
[43] P.D. Ross, A.P. Minton, Analysis of non ideal behavior in concentrated hemoglobin solutions, J. Mol. Biol. 112 (1977) 437–452.
[44] J. Behlke, O. Ristau, A new approximate whole boundary solution of the Lamm equation for the analysis of sedimentation experiments, Biophys. Chemist. 95 (2002) 59–68.
[45] B. Schiffler, M. Kiefer, A. Wilken, F. Hannemann, H.W. Adolph, R. Bernhardt, The interaction of bovine adrenodoxin with CYP11A1 (cytochrome P450scc) and CYP11B1 (cytochrome P45011β). Acceleration of reduction and substrate conversion by site-directed mutagenesis of adrenodoxin, J. Biol. Chem. 276 (2001) 36225–36232.